J. Eur. Opt. Society-Rapid Publ. 2025, **21**, 17

https://doi.org/10.1051/jeos/2025013
Available online at: https://jeos.edpsciences.org

EOSAM 2024
Guest editors: Luca De Stefano and Raffaele Velotta

Journal of the European Optical Society-Rapid Publications

RESEARCH ARTICLE

OPEN ACCESS

Beyond the IFTA – Phase mask generation for 3D laser beam shaping, tailored temperature distributions and optical amplifiers

Oskar Hofmann[1,a,*], Paul Buske[1,a], Robin Kurth[1,a], Annika Bonhoff[1], and Carlo Holly[1,2]

[1] Chair for Technology of Optical Systems (TOS) – RWTH Aachen University, Steinbachstr. 15, 52074 Aachen, Germany
[2] Fraunhofer Institute for Laser Technology (ILT), Steinbachstr. 15, 52074 Aachen, Germany

Received 31 January 2025 / Accepted 25 March 2025

Abstract. The iterative Fourier transform algorithm (IFTA) is the most widely used algorithm for the generation of phase masks for laser beam shaping in the field of laser material processing. But its simplicity and efficiency also come with heavy limitations. We here present an overview of our research into application adapted laser beam shaping beyond the capabilities of traditional phase retrieval algorithms for beam shaping. The presented algorithms enable, among others, the explicit optimization of phase masks for the generation of target light volumes and for tailored temperature distributions within a work piece. Furthermore, we demonstrate the consideration and pre-compensation of non-linear effects in an optical amplifier for laser beam shaping with subsequent amplification.

Keywords: Beam shaping, Phase retrieval, Phase mask, Non-linear amplification, Inverse heat conduction problem.

Nomenclature

IFTA	Iterative Fourier Transform Algorithm
DOE	Diffractive Optical Element
SLM	Spatial Light Modulator
LCoS	Liquid Crystal on Silicon
DNN	Diffractive Neural Network
IWPA	Iterative Wave-optical Propagation Algorithm
DHCP	Direct Heat Conduction Problem
IHCP	Inverse Heat Conduction Problem

1 Introduction

Laser beam shaping, i.e. the targeted modification of the intensity profile of a laser beam on a target plane or inside a volume, has a wide variety of applications in research and industrial use. For example, in the field of laser material processing, process adapted intensity distributions enable a targeted energy input into the work piece to achieve desired temperature distributions, phase transitions or ablation results [1–3]. A variety of beam shaping technologies are employed to achieve the required energy redistribution within a laser beam from the output of a given laser source to the desired intensity distribution: For static laser beam shaping, freeform optics [4, 5] and diffractive optical elements (DOEs) [6, 7] in particular have become well established and enable the generation of practically any physically possible intensity distribution. For dynamically switchable beam shaping elements, also known as spatial light modulators (SLMs) [8, 9], the so-called liquid crystal on silicon (LCoS) technology is currently the de-facto standard for laser applications [9, 10].

LCoS-SLMs imprint a locally varying phase modulation (phase mask) onto the incoming beam which, if chosen correctly, diffracts the beam into the desired intensity distribution in a plane behind the LCoS-SLM. However, the determination of a suitable phase mask for a given beam shaping task is usually an ill-posed problem. The transformation of a given input beam into a target intensity distribution may not be possible at all, i.e. no solution exists. And if a solution exists, there are always infinitely many solutions as the phase in the target plane remains a free parameter [11–14]. To find *one* solution, if one exists, so-called phase retrieval algorithms are used. The iterative Fourier transform algorithm (IFTA), also called Gerchberg-Saxton algorithm, is probably the most widely used phase retrieval algorithm in the field of spatial laser beam shaping [15, 16].

The main assumption for the IFTA is that the wave-optical propagation of the beam from the phase mask to the target plane can be described with a single Fourier transform of the complex electric field [6, 17]. This is based on the Fourier transform relation between a plane in front

[a] These authors contributed equally to this work.
* Corresponding author: oskar.hofmann@tos.rwth-aachen.de

of an ideal lens and the focal plane behind the lens in the Fresnel approximation of wave-optics [18]. As (discrete) Fourier transforms can be calculated numerically very efficiently [19], this enables the simulation of the light diffraction behind the phase mask with limited computational effort. Since the initial publication of the IFTA, more sophisticated algorithms for phase retrieval have been published, mostly based on the original IFTA approach [6, 15, 17]. Still, the original IFTA remains the default approach in many applications in research and industry due to its simple implementation and its independence from additional algorithms for the simulation of wave-optical light propagation.

When considering optical systems for laser beam shaping, one disadvantage of this ongoing use of the IFTA and related algorithms is a limitation regarding the positioning of the target plane. Even though the focal plane of a lens is generally not an optimal choice for the position of the target plane for laser beam shaping, the focal plane of a focusing lens (or a plane conjugate to the focal plane) remains the typical choice for beam shaping systems [20–22]. Additionally, optical elements or non-linear effects between the phase mask and the target plane can also not be considered with IFTA-based approaches.

We here present an overview of our research on phase retrieval algorithms for laser beam shaping to overcome the limitations of IFTA-based approaches with a focus on beam shaping for laser material processing. In Section 2, we discuss our approach of replacing the Fourier transform in the IFTA with a full wave-optical propagation through arbitrary optical systems. This enables a flexible positioning of the target plane and the use of additional optical elements. In Section 3, we demonstrate the use of the new algorithm for the consideration of non-linear effects from optical amplifiers for laser beam shaping with subsequent amplification. In Section 4, we present our approach of coupling the aforementioned algorithm with a solver for the so-called inverse heat conduction problem for tailored temperature distributions within a work piece. And in Section 5, we give an overview of our research into diffractive neural networks (DNNs). DNNs allow to utilize the advances in machine learning of the last decade to optimize phase masks for, among others, high fidelity 2D and 3D laser beam shaping.

2 Iterative wave-optical propagation algorithm

To overcome the limitations of the single Fourier transform in IFTA-based phase retrieval algorithms, we implement a full wave-optical simulation of the light propagation between the phase mask and the target plane (cf. Fig. 1). We keep the remaining iterative structure of the IFTA and refer the reader to the literature for further details regarding the IFTA-like structure [15, 17, 21]. In reference to the IFTA, we denote our algorithm in the following as the iterative wave-optical propagation algorithm (IWPA).

For the simulation of the wave-optical propagations we use the OPT software package developed at the Fraunhofer Institute for Laser Technology [23]. OPT consists of a collection of C^{++} and Python classes for physical-optical simulations of light propagation and optical amplifiers including non-linear amplification and thermally induced optical effects. The wave-optical free-space propagation of light is simulated with OPT by solving the Fresnel diffraction integral [24]. Propagation through optical elements, such as lenses or phase masks, is calculated in OPT in the thin element approximation [18]. The remaining IWPA is implemented in Python with a high-level interface for the calculation of the light propagation. This allows a simplified exchange of the simulation algorithm for e.g. comparisons of the results using OPT or a simple Fourier transform.

As OPT allows to model practically arbitrary optical systems, one main advantage of the IWPA is the ability to position the target plane in front or behind the focal plane of a focusing lens or do not use a focusing lens at all. This prevents the need for phase masks with large phase gradients to counteract the focusing power of the lens when creating extended intensity distributions [20, 21]. Large phase gradients are especially disadvantageous when using beam shaping elements like LCoS-SLMs that inherently suffer from pixel crosstalk [25–27].

Replacing the single Fourier transform of the IFTA with a Fresnel diffraction integral for arbitrary or multiple target planes is not a new concept and is discussed in the literature for a variety of different approaches [28–30]. It is also applied for phase retrieval in more complex optical systems consisting of multiple apertures and optical elements [31]. However, to our knowledge, these concepts are rarely or never used in the field of laser material processing. The IWPA also allows us to implement the compensation of non-linear effects in optical amplifiers as discussed in the following section.

3 Beam shaping with subsequent amplification

The IWPA also enables the calculation of phase masks for laser beam shaping with subsequent amplification. Beam shaping before passing the beam through an optical amplifier has two main advantages: Firstly, an adapted intensity distribution within the amplifier allows to improve the energy extraction from the active medium within the amplifier [32]. And secondly, moving the beam shaping element before the amplification step allows laser beam shaping at resulting laser powers and intensities beyond the damage threshold of the used beam shaping element. The damage thresholds of commercially available SLMs continue to rise but even “high power handling” SLMs still have damage thresholds well below 1 kW [33], while the laser power used in many industrial applications lies in the multi-kilowatt range [34, 35]. However, for target planes behind the optical amplifier, the influence of the amplifier (e.g. the generally non-linear amplification) must be considered and pre-compensated for by the beam shaping element. To our knowledge, such a pre-compensation in an optical system with an SLM followed by an optical amplifier was only investigated for single homogeneous target distributions, whereby the beam shaping element was additionally

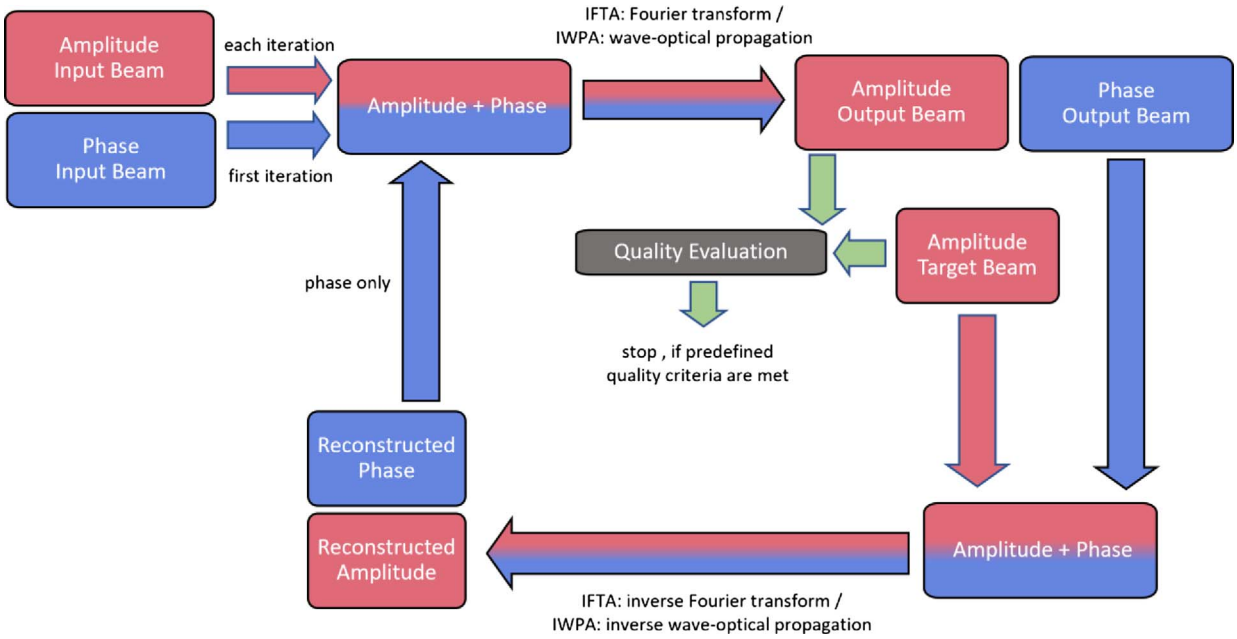

Figure 1. Flow chart of the iterative Fourier transform algorithm (IFTA) and the iterative wave-optical propagation algorithm (IWPA). The IFTA uses a forward/inverse Fourier transform to calculate the forward/inverse propagation of light through the optical system while the IWPA calculates a full (inverse) wave-optical propagation of the light.

controlled via a camera-based control loop [36, 37]. As OPT allows to simulate the spatially resolved non-linear amplification within the optical amplifier, the IWPA enables the compensation of the amplifier influence for arbitrary target distributions provided the amplifier is sufficiently characterized and the target distribution can be realized in conjunction with the optical amplifier.

To demonstrate this effect, we present simulation results for a simplified 2*f*-setup with a focal length $f = 200$ mm (cf. Fig. 2). An ideal amplifier is placed halfway between the phase mask and the focusing lens. The target plane is positioned in the focal plane of the focusing lens to allow a comparison with a phase mask calculated via IFTA. The target intensity distribution is a homogeneous distribution developed to increase the achievable surface rates for laser polishing (cf. Fig. 3) [38]. The amplification of the input beam $I_{\mathrm{in}}(x, y)$ is modeled as

$$I_{\mathrm{out}}(x,y) = I_{\mathrm{S}} \cdot W\left(\frac{G_0 \cdot \exp\left(I_{\mathrm{in}}(x,y)/I_{\mathrm{S}}\right) \cdot I_{\mathrm{in}}(x,y)}{I_{\mathrm{S}}}\right) \tag{1}$$

with the lateral coordinates (x, y), the output beam I_{out}, the saturation intensity I_{S} and the small signal gain G_0 [39, 40]. $W(x)$ denotes the Lambert W function. The amplifier is assumed to be a Nd:YAG-crystal with saturation intensity $I_{\mathrm{S}} = 20$ W/mm^2 and a small signal gain $G_0 = 5$ [41, 42]. The original input beam in front of the phase mask is a Gaussian beam with a diameter ($1/e^2$ intensity) of 6 mm and a power of 100 W. Note that the input beam I_{in} in equation (1) is the beam as it is diffracted by the phase mask onto the amplifier at a distance of $f/2$ behind the phase mask and is not simply assumed to be the original Gaussian input beam. The phase mask, amplifier and the focusing lens are simulated with a field size of 12.8 mm × 12.8 mm with a resolution of 1023 × 1023 pixels. The pixel number stems from implementation details of the IWPA via OPT (cf. Sect. 2) that are optimized for pixel counts along each dimension of $2^n - 1$, $n \in \mathbb{N}$. The target plane is simulated with a field size of 1.5 mm × 1.5 mm with the same pixel count. The phase levels of the phase mask are continuous, i.e. no discretization to the phase levels was applied.

Figure 4 compares the simulated beam shaping results for phase masks calculated via IFTA and IWPA respectively for the optical setup in Figure 2. The corresponding phase masks are shown in Figure 5. For both phase masks, the resulting intensity distribution is simulated with OPT for the optical setup with optical amplifier. As the IFTA cannot consider the amplifier, the resulting phase mask leads to a superelevation at the edges of the intensity distribution. This is caused by the non-linear amplification (Eq. (1)) that leads to a higher relative amplification for the lower intensities at the edge of the input beam compared to the center of the beam. The IWPA can take the amplifier into account and calculates a phase mask that pre-compensates for the subsequent non-linear amplification. The resulting intensity distributions are evaluated based on their normalized root mean square deviation (RMSD) from the target intensity distribution I_{target}:

$$\mathrm{RMSD} = \frac{1}{\max(I_{\mathrm{target}})} \cdot \sqrt{\frac{1}{N}\sum_n \left(I_n - I_{\mathrm{target},n}\right)^2}. \tag{2}$$

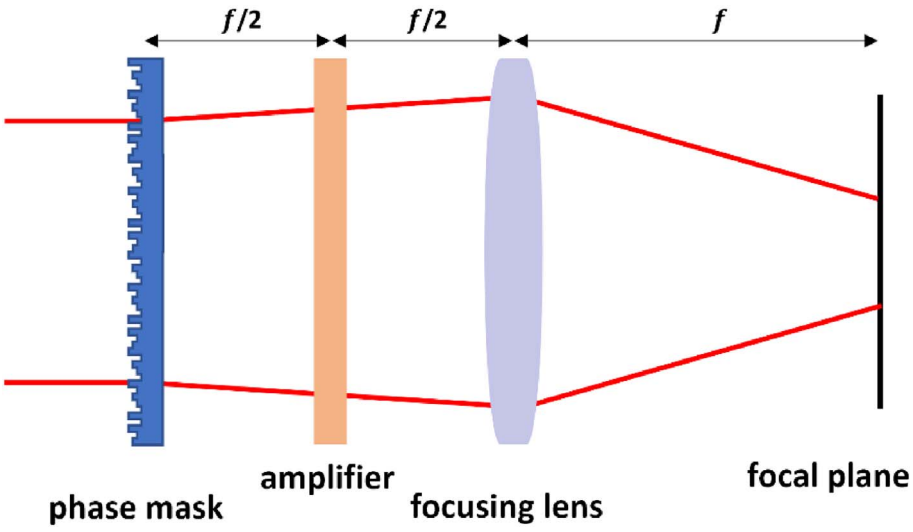

Figure 2. Schematic illustration of an ideal optical system for laser beam shaping with subsequent amplification.

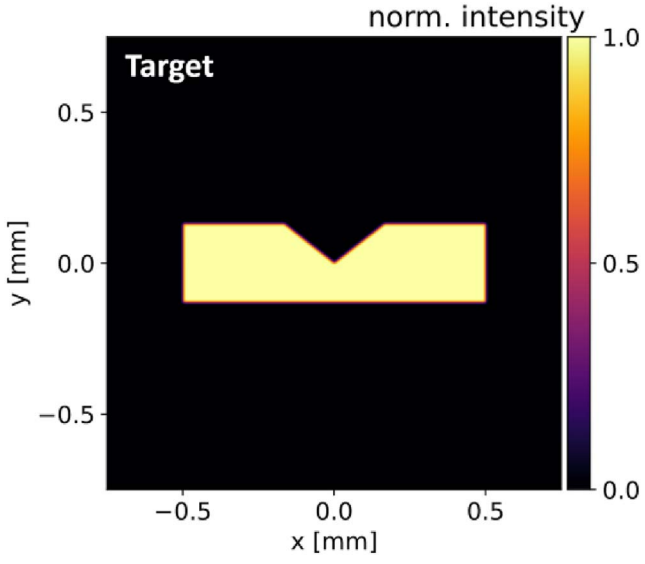

Figure 3. Selected target intensity distribution for laser beam shaping with subsequent amplification.

Here, n denotes the index of a pixel in the target intensity distribution or the simulation result, N is the total number of pixels and I_n and $I_{\text{target},n}$ are the intensities in the n-th pixel in the simulation result and in the target distribution respectively. The RMSD value heavily depends on the area in the target plane that is used for the evaluation of the RMSD. For pixels outside of the actual target distribution, both the target and the actual pixel value are usually close to zero. As the RMSD calculates a *mean* deviation, a larger evaluation area generally leads to lower RMSD values. For the results shown here, the evaluation area for the RMSD is the same as the simulated and depicted field size, i.e. 1.5 mm × 1.5 mm.

The experimental verification of these simulation results is currently in progress and will be reported in a forthcoming publication.

4 Phase mask design for tailored temperature distributions

As most material processing applications are governed by the resulting temperature distribution in the work piece, it is crucial to determine intensity distributions that result in the desired temperature distributions for the respective process. The temperature distribution resulting from a given intensity distribution can be calculated by solving the direct heat conduction problem (DHCP). The calculation of the intensity distribution that results in a given temperature distribution, however, requires to solve the ill-posed and much more complex inverse heat conduction problem (IHCP). Bonhoff implemented an iterative algorithm to solve the IHCP for a given temperature distribution, material and process parameters and experimentally verified the performance of the algorithm for laser-based softening of steel and laser hardening [2, 43, 44].

Given a target intensity distribution from solving the IHCP, the IWPA, or a different phase retrieval algorithm, can then be used to calculate a phase mask that creates the desired intensity distribution. However, even in simulations, there always remains a finite difference between the target intensity distribution and the intensity distribution resulting from the calculated phase mask (cf. Fig. 4, right). This difference depends on the complexity of the target intensity distribution and is partly caused by the finite number of pixels of the used SLM. While this difference may be the global minimum that is achievable with the given number of SLM pixels, it does not necessarily result in the smallest achievable deviation from the target

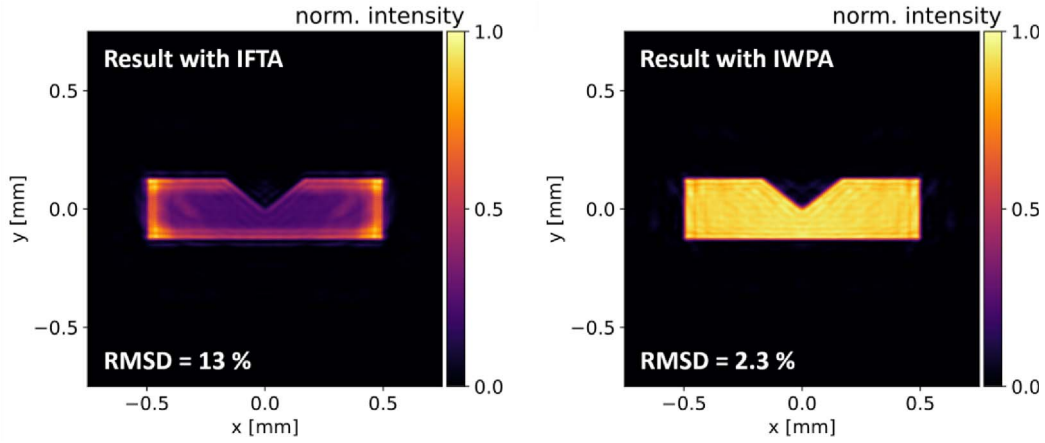

Figure 4. Simulation results for beam shaping with subsequent amplification using phase masks calculated via the iterative Fourier transform algorithm (IFTA) and the iterative wave-optical propagation algorithm (IWPA). RMSD denotes the normalized root mean square deviation from the target intensity distribution.

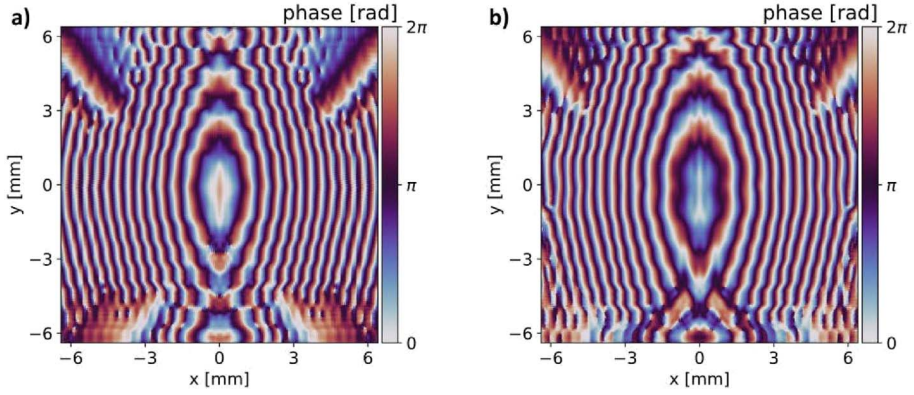

Figure 5. Corresponding phase masks for the intensity distributions shown in Figure 4. (a) Phase mask calculated via IFTA without consideration of the non-linear amplification; (b) Phase mask calculated via IWPA with consideration and compensation for the non-linear amplification.

temperature distribution. As the temperature distribution non-linearly depends on the intensity distribution, a larger deviation from the target intensity distribution can result in a smaller deviation from the target temperature distribution.

To directly optimize for a minimal deviation regarding the target temperature distribution we coupled the IWPA with our IHCP solver (cf. Fig. 6). In each iteration step, the DHCP is solved to calculate the resulting temperature field based on the current intensity distribution in the target plane. Based on the difference to the target temperature field a new adapted temperature field is calculated. The IHCP solver then calculates a new target intensity distribution for the adapted temperature field which is fed back to the normal IWPA iteration. The calculation of the adapted temperature field is required as the algorithm would otherwise always use the "normal" IHCP result for the target temperature field leading to the aforementioned minimal deviation from the resulting *intensity* distribution. The adapted temperature field, when chosen correctly, allows to push the algorithm out of minima regarding deviations from the target intensity and towards or into minima regarding the deviation from the target temperature. One approach to calculate the adapted temperature field is to overcompensate the remaining differences between the current and the target temperature field. This approach is already being used successfully to adjust target *intensity* distributions to improve the convergence for the IFTA and IWPA [6, 21].

We are currently in the process of verifying the results of this algorithm and plan to publish the results together with a more detailed description of the algorithm in an upcoming publication.

5 Diffractive neural networks

Diffractive neural networks (DNNs) are a physical equivalent to artificial neural networks in the field of machine learning. Each optical element represents a layer in the

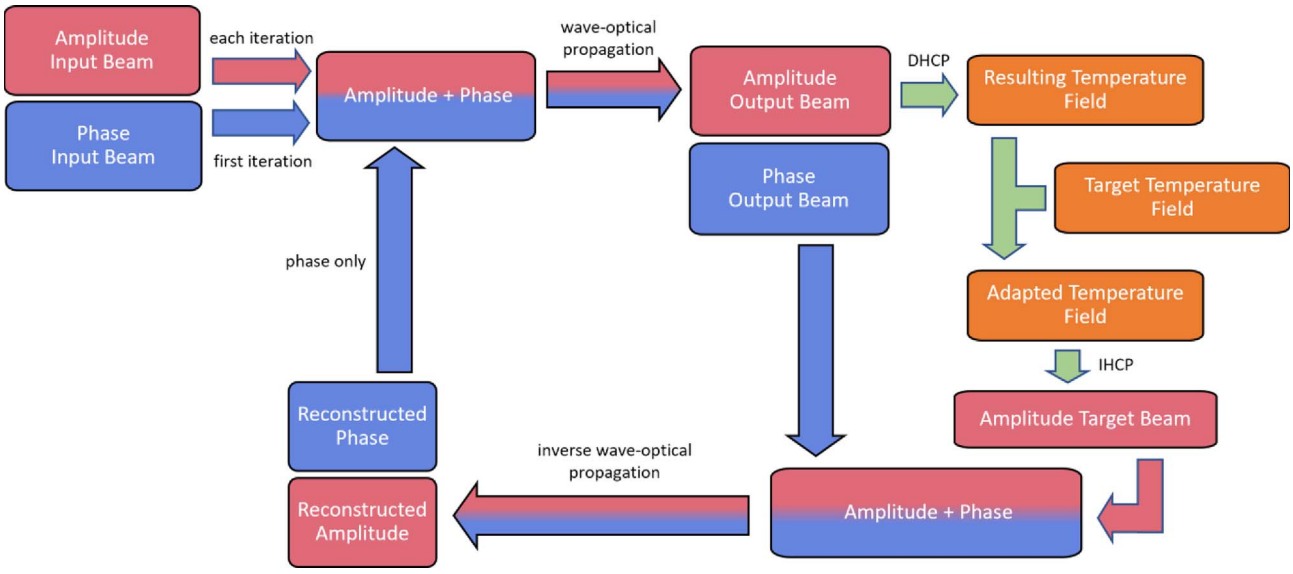

Figure 6. Flow chart of the iterative wave-optical propagation algorithm (IWPA) coupled with a solver for the direct heat conduction problem (DHCP) and the inverse heat conduction problem (IHCP) to minimize the deviation from a given target temperature field. The algorithm stops after a set number of iterations or when the difference between the resulting temperature field and the target temperature field is below a predefined value (cf. Fig. 1).

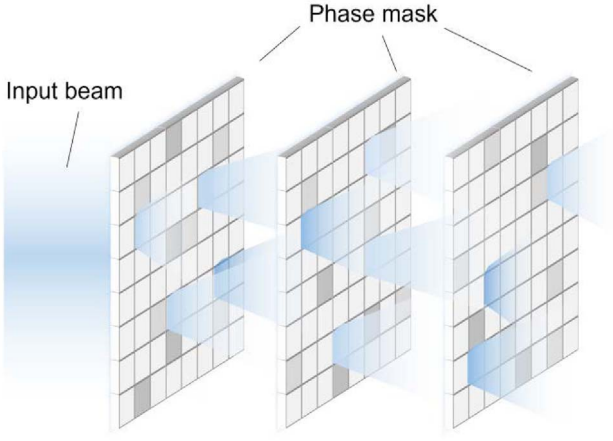

Figure 7. Schematic representation of light propagation through a diffractive neural network with three pixelated phase masks as network layers.

neural network and the layers are (fully) connected via the wave-optical propagation of light in the optical system (cf. Fig. 7). Initially developed for optical computing, DNNs allow to solve classical machine vision tasks at the speed of light [45, 46]. In the field of beam shaping, DNNs have been used for the shaping of tophat distributions with terahertz radiation and for multi-directional beam steering [47, 48].

We developed a framework to extend the area of application of DNNs to laser beam shaping with DOEs and/or LCoS-SLMs for laser material processing. By implementing the training structure for the DNNs in PyTorch Lightning, we are able to utilize the rapid advances in machine learning technology of the last decades for high fidelity laser beam shaping [22, 49]. Like the IWPA, DNNs can be used for practically arbitrary optical systems (cf. Sect. 2). DNNs also enable to simultaneously optimize two or more phase masks in an optical system and therefore provide full amplitude and phase control of the complex electric field. This allows for the direct optimization of 3D light fields with e.g. different complex intensity distributions in different target planes and intensity distributions with increased depth of field [49, 50]. Akin to neural networks for classification tasks, DNNs can also be trained to generate a constant output for similar but varying input values. This allows to create optical systems that are robust to changes of the input beam or misalignments of elements in the optical system [49, 51]. Finally, DNNs allow to consider and compensate for technology dependent influences like pixel crosstalk in LCoS-SLMs (cf. Fig. 8) [22].

Further details on the implementation and application of DNNs are outside of the scope of this overview and we refer the reader to [22, 49–51].

6 Conclusion

Laser beam shaping allows to tailor the spatial energy distribution of a laser beam to the specific application. The use of beam shaping elements based on the phase manipulation of an incoming laser beam requires so-called phase retrieval algorithms to determine suitable phase manipulations (phase masks) for a given beam shaping task. Well established phase retrieval algorithms like the iterative Fourier transform algorithm (IFTA), however, impose heavy limitations on the beam shaping system. IFTA-based approaches set the target plane for laser beam shaping to the focal plane behind a focusing lens or a plane

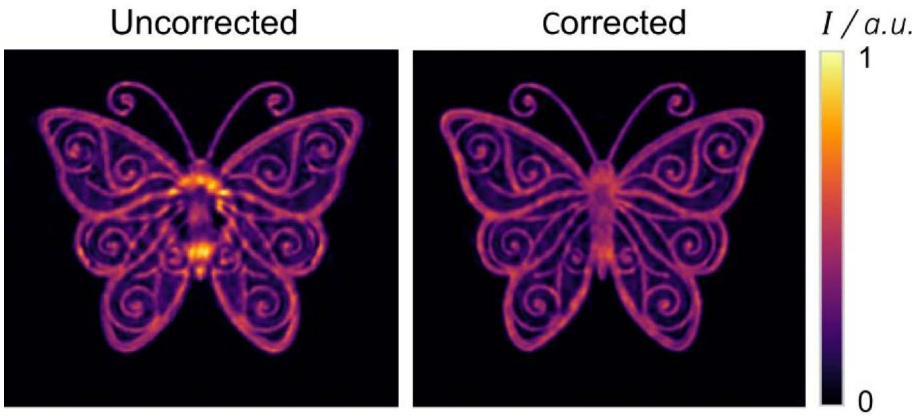

Figure 8. Example measurements of the beam shaping results with an LCoS-SLM. Left: The LCoS-SLM is modelled as an ideal phase mask but effects like pixel crosstalk lead to deviations in the displayed phase mask with a corresponding deterioration in the final intensity distribution. Right: Pixel crosstalk, astigmatism and a partial reflection at the cover glass of the LCoS-SLM are considered with a DNN and compensated for in the calculation of the phase mask.

conjugate to that focal plane. While this simplifies the implementation and calculation of the wave-optical propagation between phase mask and target plane, it often leads to suboptimal choices of optical systems for a given beam shaping task.

The iterative wave-optical propagation algorithm (IWPA) is an adaptation of the IFTA that keeps the iterative structure of the IFTA but simulates the (inverse) wave-optical propagation of light through an arbitrary optical system. One advantage of the IWPA is the possibility to freely position the target plane for laser beam shaping, thus eliminating the restriction to the focal plane of a focusing lens imposed by the IFTA. We also demonstrate the use of the IWPA for laser beam shaping with subsequent amplification based on the ability of the IWPA to consider non-linear effects in the optical system. Additionally, we present an approach to calculate phase masks that minimize the deviation from a target temperature distribution in a work piece by coupling the IWPA with a solver for the inverse heat conduction problem.

Diffractive neural networks are a physical representation of artificial neural networks and enable the use of established machine-learning approaches for high fidelity laser beam shaping. DNNs enable to design an optical system with two or more phase masks for full amplitude and phase control of the laser beam. This allows for the direct optimization of 3D light fields and for phase mask design that is robust against changes of the input beam or misalignments in the optical system. DNNs also enable phase mask design that compensates for properties of the chosen beam shaping element like pixel crosstalk in liquid crystal on silicon spatial light modulators.

When selecting a suitable optical system and a phase retrieval algorithm for a specific beam shaping task, all alternatives should therefore be considered and weighed against each other. IFTA-based approaches offer relatively easy integration combined with strict limitations regarding the optical system and often limited achievable quality of the beam shaping results. Approaches like the here presented IWPA and DNN require additional effort in their implementation compared to an IFTA, but offer a higher flexibility in terms of suitable optical systems and often enable a higher fidelity in the achievable beam shaping results.

Funding

The presented work was funded by the Deutsche Forschungsgemeinschaft (DFG, German Research Foundation) – LO 640/20-1, 387868000, and EXC-2023 Internet of Production - 390621612. Oskar Hofmann was part of the Max Planck School of Photonics supported by BMBF, Max Planck Society, and Fraunhofer Society. This research was completed within the European Union project METAMORPHA. The METAMORPHA project has received funding from Horizon Europe, the European Union's Framework Programme for Research and Innovation, under grant agreement 101057457. Views and opinions expressed are however those of the authors only and do not necessarily reflect those of the European Union. The European Union cannot be held responsible for them.

Conflicts of interest

The authors have nothing to disclose.

Data availability statement

Data underlying the results presented in this paper are not publicly available at this time but may be obtained from the authors upon reasonable request.

Author contribution statement

Conceptualization, O.H.; Methodology, O.H., P.B., R.K., A.B. and C.H.; Software, O.H., P.B., R.K., and A.B.; Validation, O.H., P.B. and R.K.; Formal Analysis, O.H., P.B., R.K., A.B. and C.H.; Investigation, O.H., P.B. and R.K.; Resources, A.B. and C.H.; Data Curation, O.H., P.B. and R.K.; Writing – Original Draft Preparation, O.H.; Writing – Review & Editing, P.B., R.K., A.B. and C.H.; Visualization, O.H. and P.B.; Supervision, O.H., A.B. and C.H.; Project Administration, O.H., A.B. and C.H.; Funding Acquisition, O.H., A.B. and C.H.

References

1 González AB, Pozo J, Optical beam shaping: unmet needs in laser materials processing, *Optik Photonik* **12**, 15–17 (2017).
2 Völl A, Vogt S, Wester R, Stollenwerk J, Loosen P, Application specific intensity distributions for laser materials processing: Tailoring the induced temperature profile, *Opt. Laser Technol.* **108**, 583–591 (2018).
3 Bischoff C, Völklein F, Schmitt J, Rädel U, Umhofer U, Jäger E, Lasagni AF, Design and manufacturing method of fundamental beam mode shaper for adapted laser beam profile in laser material processing, *Materials (Basel, Switzerland)* **12**, 2254 (2019).
4 Feng Z, Huang L, Gong M, Jin G, Beam shaping system design using double freeform optical surfaces, *Opt. Express, OE* **21**, 14728–14735 (2013).
5 Völl A, Wester R, Berens M, Buske P, Stollenwerk J, Loosen P, Accounting for laser beam characteristics in the design of freeform optics for laser material processing, *Adv. Opt. Technol.* **8**, 279–287 (2019).
6 Liu JS, Taghizadeh MR, Iterative algorithm for the design of diffractive phase elements for laser beam shaping, *Opt. Lett.* **27**, 1463–1465 (2002).
7 O'Shea DC, Suleski TJ, Kathman AD, Prather DW, *Diffractive optics: design, fabrication, and test. Design, fabrication, and test* (SPIE, Bellingham, Washington, USA, 2003).
8 Efron U, *Spatial light modulator technology, devices and applications*, (Dekker, New York, USA, 1995).
9 Salter PS, Booth MJ, Adaptive optics in laser processing, *Light Sci. Appl.* **8**, 110 (2019).
10 Rosales-Guzmán C, *How to shape light with spatial light modulators* (Society of Photo-Optical Instrumentation Engineers (SPIE), Bellingham, Washington, USA, 2017).
11 Dickey FM, *Laser beam shaping: Theory and techniques*, 2nd edn. (CRC Press, Boca Raton, Florida, USA, 2014).
12 Brenner K-H, Kuemmel P, Zeitner UD, Design, analysis, and fabrication of refractive beam shaping elements for optical storage applications, in *Laser Beam Shaping II*, SPIE Proceedings (SPIE, 2001).
13 Kaempfe T, Kley E-B, Tuennermann A, Hybrid approach to the design of refractive beam shaping elements, in *Laser Beam Shaping VI*, SPIE Proceedings (SPIE, 2005).
14 Lin D, Leger JR, Numerical gradient-index design for coherent mode conversion, *Adv. Opt. Technol.* **1**(3), 195–202 (2012).
15 Kim H, Yang B, Lee B, Iterative Fourier transform algorithm with regularization for the optimal design of diffractive optical elements, *J. Opt. Soc. Am. A Opt. Image Sci.* **21**, 2353–2365 (2004).
16 Gerchberg RW, Saxton WO, A practical algorithm for the determination of phase from image and diffraction plane pictures, *Optik* **35**, 237–246 (1972).
17 Fienup JR, Phase retrieval algorithms: a comparison, *Appl. Opt.* **21**, 2758–2769 (1982).
18 Goodman JW, *Introduction to Fourier optics*, 3rd edn (Roberts & Company, Englewood, Coloroda, USA, 2005).
19 Nussbaumer HJ, The fast Fourier transform, in *Fast Fourier transform and convolution algorithms*, edited by HJ Nussbaumer, **Vol. 2** (Springer, Berlin/Heidelberg, Germany, 1981).
20 Hofmann O, Stollenwerk J, Holly C, Iterative algorithm for the generation of phase masks for spatial laser beam shaping in arbitrary optical systems, in *International Optical Design Conference 2023* (SPIE, 2023).
21 Hofmann OA, *Highly dynamic multi-beam and beam shaping systems for laser material processing*, (RWTH Aachen University, 2023).
22 Buske P, Hofmann O, Bonnhoff A, Stollenwerk J, Holly C, High fidelity laser beam shaping using liquid crystal on silicon spatial light modulators as diffractive neural networks, *Opt. Express, OE* **32**, 7064–7078 (2024).
23 Wester R, Physical optics methods for laser and nonlinear optics simulations, *Adv. Opt. Technol.* **2**, 247–255 (2013).
24 Born M, Wolf E, *Principles of optics. Electromagnetic theory of propagation, interference and diffraction of light*, 7th Edn. (Cambridge University Press, Cambridge, UK, 1999).
25 Moser S, Ritsch-Marte M, Thalhammer G, Model-based compensation of pixel crosstalk in liquid crystal spatial light modulators, *Opt. Express* **27**, 25046–25063 (2019).
26 Persson M, Engström D, Goksör M, Reducing the effect of pixel crosstalk in phase only spatial light modulators, *Opt. Express* **20**, 22334–22343 (2012).
27 Ronzitti E, Guillon M, Sars V de, Emiliani V, LCoS nematic SLM characterization and modeling for diffraction efficiency optimization, zero and ghost orders suppression, *Opt. Express* **20**, 17843–17855 (2012).
28 Makowski M, Three-plane phase-only computer hologram generated with iterative Fresnel algorithm, *Opt. Eng.* **44**, 125805 (2005).
29 Gureyev T, Pogany A, Paganin D, Wilkins S, Linear algorithms for phase retrieval in the Fresnel region, *Opt. Commun.* **231**, 53–70 (2004).
30 Zalevsky Z, Mendlovic D, Dorsch RG, Gerchberg-Saxton algorithm applied in the fractional Fourier or the Fresnel domain, *Opt. Lett.* **21**, 842–844 (1996).
31 Fienup JR, Phase-retrieval algorithms for a complicated optical system, *Appl. Opt.* **32**, 1737–1746 (1993).
32 Adamonis J, Aleknavičius A, Michailovas K, Balickas S, Petrauskienė V, Gertus T, Michailovas A, Implementation of a SVWP-based laser beam shaping technique for generation of 100-mJ-level picosecond pulses, *Appl. Opt.* **55**, 8007–8015 (2016).
33 Hamamatsu Photonics, *X15213-03CL. LCOS-SLM (Optical phase modulator)* (Hamamatsu Photonics, 2024). https://www.hamamatsu.com/us/en/product/optical-components/lcos-slm/metal_processing_type/X15213-03CL.html.
34 Shiner B, Fiber lasers for material processing, in: *Critical Review: Industrial Lasers and Applications*, SPIE Proceedings (SPIE, 2005).
35 Vukovic N, Chan JS, Codemard CA, Zervas MN, Keen SJ, Chen R, Jesset R, Botheroyd I, Durkin M, Greenwood M, Multi-kilowatt fibre laser with azimuthal mode output beam for advanced material processing, in: *Laser Resonators, Microresonators, and Beam Control XXII*, (SPIE, 2020).
36 Zhao T, Yu J, Li C, Huang K, Ma Y, Tang X, Fan Z, Beam shaping and compensation for high-gain Nd:glass amplification, *J. Modern Optics* **60**, 109–115 (2013).
37 Li S, Wang Y, Lu Z, Ding L, Du P, Chen Y, Zheng Z, Ba D, Dong Y, Yuan H, Bai Z, Liu Z, Cui C, High-quality near-field beam achieved in a high-power laser based on SLM adaptive beam-shaping system, *Opt. Express* **23**, 681–689 (2015).
38 Kumstel J, Enhancement of the area rate for laser macro polishing, in: *Lasers in Manufacturing LIM* (2017).
39 Koechner W, *Solid-State Laser Engineering*, 6th Edn., (Springer e-books, Springer New York, New York, USA, 2006).

40 Ter-Mikirtychev V, *Fundamentals of fiber lasers and fiber amplifiers* (Springer International Publishing, Charm, Switzerland, 2014).

41 Fuhrmann K, Hodgson N, Hollinger F, Weber H, Effective cross section of the Nd:YAG 1.0641-µm laser transition, *J. Appl. Phys.* **62**, 4041–4044 (1987).

42 Park D, Jeong J, Hwang S, Lee S, Cho S, Yu TJ, Performance evaluation of solid-state laser gain module by measurement of thermal effect and energy storage, *Photonics* **8**, 418 (2021).

43 Völl A, Stollenwerk J, Loosen P, Computing specific intensity distributions for laser material processing by solving an inverse heat conduction problem, in *High-power laser materials processing: lasers, beam delivery, diagnostics, and applications V*, SPIE Proceedings (SPIE, 2016).

44 Völl A, *Methodology for the identification and implementation of application specific intensity distributions for material processing with laser radiation* (RWTH Aachen University, 2020).

45 Lin X, Rivenson Y, Yardimci NT, Veli M, Luo Y, Jarrahi M, Ozcan A, All-optical machine learning using diffractive deep neural networks, *Science (New York, N.Y.)* **361**, 1004–1008 (2018).

46 Yan T, Wu J, Zhou T, Xie H, Xu F, Fan J, Fang L, Lin X, Dai Q, Solving computer vision tasks with diffractive neural networks, in: *Optoelectronic Imaging and Multimedia Technology VI* (SPIE, 2019).

47 Shi J, Wei D, Hu C, Chen M, Liu K, Luo J, Zhang X, Robust light beam diffractive shaping based on a kind of compact all-optical neural network, *Opt. Express, OE* **29**, 7084–7099 (2021).

48 Idehenre IU, Mills MS, Multi-directional beam steering using diffractive neural networks, *Opt. Express, OE* **28**, 25915–25934 (2020).

49 Buske P, Völl A, Eisebitt M, Stollenwerk J, Holly C, Advanced beam shaping for laser materials processing based on diffractive neural networks, *Opt. Express, OE* **30**, 22798–22816 (2022).

50 Buske P, Janssen F, Hofmann O, Stollenwerk J, Holly C, Enhancing three-dimensional beam shaping accuracy through cascaded spatial light modulators using diffractive neural networks, in *Computational Optics* (SPIE, 2024).

51 Buske P, Michels L, Wahl C, Grossert C, Hofmann O, Bonhoff A, Holly C, *Diffractive neural networks with polynomial phase masks for laser beam shaping with quasi-continuous diffractive optical elements* (2025).